View Article Online / Journal Homepage / Table of Contents for this issue
Dynamic Article Links

Nanoscale

Cite this: *Nanoscale*, 2011, **3**, 974

www.rsc.org/nanoscale

COMMUNICATION

Sol–gel nanocasting synthesis of patterned hierarchical $LaFeO_3$ fibers with enhanced catalytic CO oxidation activity†

Pengna Li,[a] Xianluo Hu,*[b] Lei Zhang,[c] Hongxing Dai*[c] and Lizhi Zhang*[a]

Received 12th October 2010, Accepted 13th December 2010
DOI: 10.1039/c0nr00760a

Published on 14 January 2011. Downloaded by Fail Open on 7/23/2025 10:02:12 AM.

Hierarchical $LaFeO_3$ fibers were prepared by a sol–gel nanocasting method using a cotton cloth as the template. The resulting $LaFeO_3$ fibers inherited the initial network morphology of the template very well and showed enhanced catalytic CO oxidation activity and satisfactory stability compared to the counterpart particles prepared by the conventional sol–gel method.

The development of nanomaterials with novel structures has opened new opportunities in exploring their widely varying properties. Many methods have been applied to build controlled or tailored nanostructures. Among them, nanocasting is a versatile method for creating organized and mesostructured materials based on replicating nanoscale structures *via* a direct-templating process.[1] Various morphologies, *e.g.,* nanowires, nanoarrays and nanospheres have been obtained by the strategy of "nanocasting",[2,3] and many templates can be used in the nanocasting procedure. It is well known that nature is full of materials with sophisticated structure and ordering, which could serve as diverse templates for replication to design and fabricate target inorganic materials with predetermined structural properties. These natural templates include bacterial superstructures,[4] cotton/cloth textile,[5] diatoms,[6] dog and human hair,[7] living cells,[7] mushroom gills,[8] shell membrane,[8] silk fiber,[7] skeletal plates,[8] spider silk,[7] and so on. With the assistance of templates, the as-fabricated nanoscale products not only inherit the related properties from their individual parents, but also provide the possibility for enhanced functionality.[9]

CO is a major pollutant which forms due to incomplete combustion of gasoline in automotive engines. Its oxidation becomes an essential issue for air purification, automotive emission control, and so on. Nanosized Au is the most effective catalyst for reducing the emission levels of CO.[10] However, it is very expensive and easily deactivated by Pb and P, which limits the industrial use. Therefore, many researchers have attempted to develop a catalyst with relatively low cost and better poison resistance to replace the noble metal Au catalyst. Under such a background, perovskite-type oxides (ABO_3) containing transition metals (*e.g.,* Co, Mn, Fe, *etc.*) began to attract considerable attention several decades ago because of their high catalytic activity and good thermal stability. In 1952, perovskites were first used as catalytic materials for CO oxidation.[11] Twenty years later, their potential application as a catalyst for automobile exhaust purification was reported by Libby.[12] Among the various ABO_3 materials, $LaFeO_3$ and the related compounds become very promising for their potential applications including catalysts,[13] membranes in syngas production,[14] sensors,[15,16] and environmental monitoring materials. Recently, $LaFeO_3$ was found to exhibit attractive catalytic activity in the destruction of chlorinated volatile organic compounds (VOCs).[17]

In this communication, we demonstrate for the first time a sol–gel nanocasting route to the synthesis of perovskite-type oxide $LaFeO_3$ by using a cotton cloth as the template. This method allows the successful creation of large-scale patterning of the hierarchical $LaFeO_3$ fibers. The reaction proceeds at atmospheric pressure and the method is facile and low cost. The catalytic performance of the resulting hierarchical $LaFeO_3$ fibers for the oxidation of CO is investigated and compared with that of the conventional sol–gel synthesized $LaFeO_3$ nanoparticles.

The structure of $LaFeO_3$ fibers and particles was characterized by XRD (see Fig. S1, ESI†). The results reveal that the calcined products were well crystallized. Both of the two XRD patterns display diffraction peaks around 2θ = 22.8, 32.4, 39.9, 46.3, 52.2, 57.6 and 67.5°, which could be indexed to the characteristic crystal planes (101), (121), (220), (202), (141), (240) and (242) of orthorhombic $LaFeO_3$ perovskite-type structure (JCPDS file no. 15-148). No other crystalline by-products were found in the patterns, indicating high purity of the products.

Fig. 1 shows the SEM images of the original template and the obtained $LaFeO_3$ fibers and particles. As shown in Fig. 1a, the cotton cloth template consists of an artificial pseudo-2D network of cotton threads in compact bundles by simple weaving. Each bundle consists of a large number of strips with widths of 20–40 μm and an average thickness of about 10 μm. Fig. 1b displays a representative overview

[a]*Key Laboratory of Pesticide & Chemical Biology of Ministry of Education, College of Chemistry, Central China Normal University, Wuhan, 430079, PR China. E-mail: zhanglz@mail.ccnu.edu.cn; Fax: + 86-27-6786 7535; Tel: + 86-27-6786 7535*
[b]*State Key Laboratory of Material Processing and Die & Mould Technology, College of Materials Science and Engineering, Huazhong University of Science and Technology, Wuhan, 430074, PR China. E-mail: huxl@mail.hust.edu.cn*
[c]*Laboratory of Catalysis Chemistry and Nanoscience, Department of Chemistry and Chemical Engineering, College of Environmental and Energy Engineering, Beijing University of Technology, Beijing, 100124, PR China. E-mail: hxdai@bjut.edu.cn*
† Electronic supplementary information (ESI) available: Materials, detailed experimental procedures and characterization, XRD patterns, SEM and TEM images, BET data and XPS spectra. See DOI: 10.1039/c0nr00760a

This journal is © The Royal Society of Chemistry 2011

View Article Online

Published on 14 January 2011. Downloaded by Fail Open on 7/23/2025 10:02:12 AM.

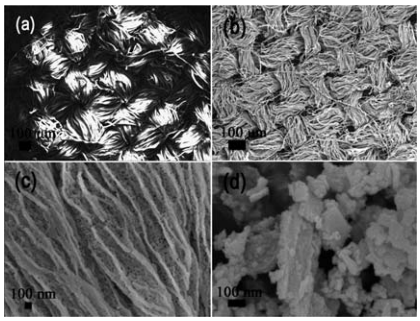

Fig. 1 SEM images of (a) original cloth, (b and c) $LaFeO_3$ fibers at different magnifications and (d) $LaFeO_3$ particles.

of the $LaFeO_3$ fibers after calcination at 650 °C. The patterning consisted of interconnected frameworks of many filaments. The resulting framework inherited the initial network of the cotton template very well, except that the dimension was shrunk. The dimension of the $LaFeO_3$ cloth was reduced by about 1/5 due to the shrinkage after template removal. The high-magnification SEM images reveal that the hierarchical cellulosic structure of $LaFeO_3$ fibers comprises subunits of numerous nanoparticles with diameters of about 30–40 nm (Fig. 1c). The interconnecting filaments were composed of fused nanoparticles and a large amount of pores formed among the nanoparticles. Fig. 1d is a representative SEM image of the $LaFeO_3$ particles prepared by conventional sol–gel method. Obviously, the conventional sol–gel synthesized product was composed of irregular aggregates of nanoparticles with about 30–200 nm in size, which was different from sol–gel nanocast $LaFeO_3$ fibers. The size and microstructure of the resulting $LaFeO_3$ fibers and particles were further investigated by means of the TEM technique (see Fig. S2, ESI†). Fig. S2a† shows a typical TEM image of sol–gel nanocast $LaFeO_3$ fibers. It is found that $LaFeO_3$ fibers were of numerous nanoparticles of about 30–40 nm in size, and the particles were quite uniform and highly aggregated. The TEM image of $LaFeO_3$ particles prepared through the conventional sol–gel method, shown in Fig. S2b†, reveals that their sizes were larger than those of the fibers. This is consistent with the SEM results in Fig. 1c and d.

The porous structures of the resulting samples were further studied by nitrogen sorption (see Fig. S3, ESI†). The adsorption isotherms of the two samples could be classified as type III with hysteresis loops, in which the adsorbate–adsorbate interactions play an important role.[18] The adsorption isotherms were typical characteristics of large mesopores and/or macropores produced by interaggregated particles. The BET surface areas of $LaFeO_3$ fibers and particles were 23 and 11 $m^2 g^{-1}$, respectively. Obviously, the surface area of the former was significantly higher than that of the latter. The inset of Fig. S3† reveals that the large mesopore and/or macropore size distribution in $LaFeO_3$ fibers is broader than that in $LaFeO_3$ particles and the overall porosity of $LaFeO_3$ fibers is higher than that of $LaFeO_3$ particles.

The surface electronic states and the composition of the samples were characterized by X-ray photoelectron spectroscopy (see Fig. S4, ESI†). In $LaFeO_3$, Fe and La atoms existed in more than one chemical states (A- or B-sites), bringing about several different contributions with different binding energies in the XPS spectra.[19] Fig. S4† shows the typical XPS spectra of $LaFeO_3$ fibers and particles. The peak positions of different atoms were determined by internally referencing the adventitious carbon at a binding energy of 284.8 eV. The survey spectra (Fig. S4a†) reveal that both the surfaces of $LaFeO_3$ fibers and particles were composed of four elements, La, O, Fe and a trace amount of C. From Fig. S4b† the La 3d core level spectrum could be observed at binding energies of around 852.3 eV (La $3d_{3/2}$) and 835.4 eV (La $3d_{5/2}$), in good agreement with that in $LaFeO_3$.[20] The satellites with higher binding energies corresponded to the shake-up state of La 3d, resulting from a core hole with an electron transferred from the O 2p valence band to an empty La 4f orbit. As shown in the spectrum in Fig. S4c†, the peaks of 710.8 and 724.1 eV could be attributed to Fe $2p_{3/2}$ and Fe $2p_{1/2}$, respectively. In O 1s spectra (Fig. S4d†), the peaks at 529.1 eV were attributed to Fe–O and La–O bonds (lattice oxygen), and the peaks at 531.5 eV were assigned to carbonates and hydroxides adsorbed on the catalyst surfaces (surface oxygen). Obviously, the surface adsorbed oxygen content in $LaFeO_3$ fibers is less than that in $LaFeO_3$ particles, suggesting the cotton cloth template could reduce the surface oxygen species. To investigate the carbon states in the two samples, we measured C 1s core levels, as shown in Fig. S4e†. The binding energies of 284.8 and 289.6 eV were observed in both $LaFeO_3$ fibers and particles. The peak (284.8 eV) is attributed to signal the presence of adventitious element carbon. The other peak (289.6 eV) indicates the presence of carbonate species which is consistent with the results in Fig. S4d†.

On the basis of the above results, we propose a possible formation processes of $LaFeO_3$ particles and fibers, as illustrated in Scheme 1. For the conventional sol–gel synthesized $LaFeO_3$ particles, citric acid first formed chelate complexes with the metal ions (Fe^{3+}, La^{3+}).[21] After hydrolysis and dehydration–condensation reactions, the sol precursor with homogenously distributed Fe and La ions was formed. The subsequent drying step would result in gel formation *via* the further condensation. The final calcination process produced irregular aggregates of $LaFeO_3$ nanoparticles because of the absence of any template. However, the formation of $LaFeO_3$ fibers is thought to be different. The first step of the sol particle formation was similar with that of the conventional sol–gel synthesized $LaFeO_3$ particles. As soon as the sol particles contacted with the cotton cloth, these particles would be adsorbed onto the cotton thread surfaces. The overnight immersion would ensure the sufficient adsorption. The adsorbed sol particles could condense into gel in the cellulose matrix of the cotton threads. The final calcination would decompose the gel and result in the formation of patterned hierarchical $LaFeO_3$ fibers by inheriting the morphology and three-dimensional architectures of cotton threads, which were burnt out simultaneously. Of course, a slight shrinkage of the overall dimensions took place at the same time due to the loss of cotton fibers.

The catalytic performance of both $LaFeO_3$ fibers and particles for the oxidation of CO was evaluated. The tests involved measuring the temperature dependent conversion of CO to CO_2 up to the points of

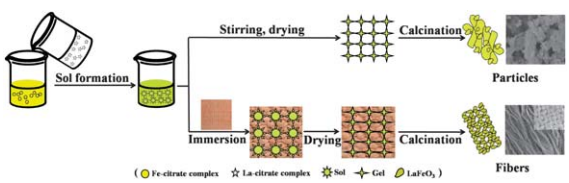

Scheme 1 Illustration of possible formation mechanism of $LaFeO_3$ particles and fibers.

View Article Online

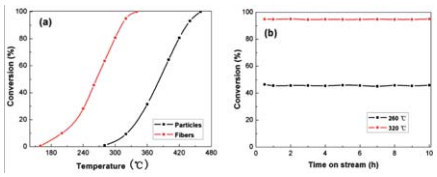

Fig. 2 (a) Conversion of CO to CO_2 *versus* temperature; (b) conversion of CO to CO_2 *versus* time on stream over the $LaFeO_3$ fibers at 260 and 320 °C, respectively.

Published on 14 January 2011. Downloaded by Fail Open on 7/23/2025 10:02:12 AM.

50% (T50, which was usually invited to express the catalytic activity) and 100% conversion (CO in the product mixture was no longer detectable by GC) and the stability of catalytic performance. We detected no oxidation of CO below 160 °C over the $LaFeO_3$ fibers and below 280 °C over the $LaFeO_3$ particles. As shown in Fig. 2a, CO conversions increased with the rise in reaction temperature, the T50 temperatures were 264 °C for $LaFeO_3$ fibers and 383 °C for $LaFeO_3$ particles, revealing the catalytic performance of the $LaFeO_3$ fibers is superior to that of the $LaFeO_3$ particles, we also observed that $LaFeO_3$ fibers and particles could completely convert CO to CO_2 at a temperature of 340 °C and 460 °C respectively, which further confirmed the excellent activity of $LaFeO_3$ fibers. Furthermore, we tested the catalytic stability of the sol–gel nanocasted $LaFeO_3$ sample over time. The fibrous $LaFeO_3$ catalyst showed satisfactory stability over 10 h both at 260 °C and 320 °C (Fig. 2b). Zhu *et al.* found the CO conversion on La_2CuO_4 prepared by the conventional citrate combustion method was less than 20% at 325 °C.[22] Tilset and his co-workers reported the temperature for 100% of CO conversion to CO_2 on $NdCoO_3$ was up to 523 °C.[23] Compared with these two perovskite-type oxides, $LaFeO_3$ fibers in this work exhibited much better catalytic performance. As revealed from the XPS analysis, the surface adsorbed oxygen content in $LaFeO_3$ fibers is less than that in $LaFeO_3$ particles. Usually, more surface oxygen species could favour the CO oxidation. So the higher CO oxidation activity of the $LaFeO_3$ fibers could not be assigned to surface oxygen species in this study. Therefore, the excellent catalytic performance is attributed to the novel structural and textural characteristics of the $LaFeO_3$ fibers prepared *via* the sol–gel nanocasting route. First, the hierarchical structure makes it easier for the reactant to access the surface active sites, so it would facilitate the CO adsorption and oxidation at the active sites as well as the product desorption. Second, the surface area of the sol–gel nanocasting synthesized $LaFeO_3$ fibers was twice as large as that of the counterpart particles. It is widely accepted that the large surface area is favorable for catalytic activity enhancement because large surface area means more active sites, allowing for the generation of more active species and the facile proceeding of CO oxidation.

In summary, we have demonstrated a facile and low cost sol–gel nanocasting strategy to produce patterned hierarchical perovskite-type oxide $LaFeO_3$ fibers by choosing a cotton cloth as the template. The resulting nanocast $LaFeO_3$ fibers inherited the initial network morphology of the template very well and possessed a larger surface area than the counterpart particles prepared by conventional sol–gel method. Furthermore, the nanocast product showed much better catalytic performance and satisfactory stability in the oxidation of CO to CO_2. We believe that this facile method could be extended to prepare other binary metal oxides with enhanced catalytic properties.

Acknowledgements

This work was supported by the National Basic Research Program of China (973 Program) (grant 2007CB613301), National Science Foundation of China (grants 20777026, 20977039, 21073069, and 91023010), the Key Project of Ministry of Education of China (grant 108097), Program for Innovation Team of Hubei Province (2009CDA048), Self-Determine Research Funds of CCNU from the Colleges' Basic Research and Operation of MOE (grants CCNU09A02014 and CCNU09C01009), and Program for New Century Excellent Talents in University (grant NCET-07-0352).

Notes and references

1 C. West and R. Mokaya, *Chem. Mater.*, 2009, **21**, 4080–4086.
2 H. F. Yang, Q. H. Shi, B. Z. Tian, Q. Y. Lu, F. Gao, S. H. Xie, J. Fan, C. Z. Yu, B. Tu and D. Y. Zhao, *J. Am. Chem. Soc.*, 2003, **125**, 4724–4725.
3 F. Zhang, Y. Wan, Y. F. Shi, B. Tu and D. Y. Zhao, *Chem. Mater.*, 2008, **20**, 3778–3784.
4 L. Chen, Y. H. Shen, A. J. Xie, B. Huang, R. Jia, R. Y. Guo and W. Z. Tang, *Cryst. Growth Des.*, 2009, **9**, 743–754.
5 S. M. Zhu, D. Zhang, Z. Q. Li, H. Furukawa and Z. X. Chen, *Langmuir*, 2008, **24**, 6292–6299.
6 J. Toster, K. S. Iyer, R. Burtovyy, S. S. O. Burgess, I. A. Luzinov and C. L. Raston, *J. Am. Chem. Soc.*, 2009, **131**, 8356–8357.
7 S. Sotiropoulou, Y. Sierra-Sastre, S. S. Mark and C. A. Batt, *Chem. Mater.*, 2008, **20**, 821–834.
8 F. C. Meldrum and H. Cölfen, *Chem. Rev.*, 2008, **108**, 4332–4432.
9 S. L. Mao, J. J. Zhao, S. Y. Zhang, H. L. Niu, B. K. Jin and Y. P. Tian, *J. Phys. Chem. C*, 2009, **113**, 18091–18096.
10 R. A. Ojifinni, N. S. Froemming, J. L. Gong, M. Pan, T. S. Kim, J. M. White, G. Graeme Henkelman and C. B. Mullins, *J. Am. Chem. Soc.*, 2008, **130**, 6801–6812.
11 G. Parravano, *J. Chem. Phys.*, 1952, **20**, 342–343.
12 W. F. Libby, *Science*, 1971, **171**, 499–500.
13 X. P. Dai, Q. Wu, R. J. Li, C. C. Yu and Z. P. Hao, *J. Phys. Chem. B*, 2006, **110**, 25856–25862.
14 S. Guntuka, S. Banerjee, S. Farooq and M. P. Srinivasan, *Ind. Eng. Chem. Res.*, 2008, **47**, 154–162.
15 D. Wang, X. F. Chu and M. L. Gong, *Nanotechnology*, 2006, **17**, 5501–5505.
16 M. Siemons, A. Leifert and U. Simon, *Adv. Funct. Mater.*, 2007, **17**, 2189–2197.
17 A. D. Paoli and A. A. Barresi, *Ind. Eng. Chem. Res.*, 2001, **40**, 1460–1464.
18 K. S. W. Sing, D. H. Everett, R. A. W. Haul, L. Moscou, R. A. Pierotti, J. Rouquerol and T. Siemieniewska, *Pure Appl. Chem.*, 1985, **57**, 603–619.
19 M. L. Wen, Q. Li and Y. T. Li, *J. Electron Spectrosc. Relat. Phenom.*, 2006, **153**, 65.
20 X. X. Guo, Z. H. Chen, D. F. Cui, Y. L. Zhou, H. Z. Huang, H. X. Zhang, F. Q. Liu, K. Ibrahim and H. J. Qian, *J. Cryst. Growth*, 2000, **219**, 404–408.
21 J. Lin, M. Yu, C. Lin and X. Liu, *J. Phys. Chem. C*, 2007, **111**, 5835–5845.
22 J. J. Zhu, Z. Zhao, D. H. Xiao, J. Li, X. G. Yang and Y. Wu, *Ind. Eng. Chem. Res.*, 2005, **44**, 4227–4233.
23 B. G. Tilset, H. Fjellvag, A. Kjekshus, A. Slagtern and I. Dahl, *Appl. Catal., A*, 1996, **147**, 189–205.

 This journal is © The Royal Society of Chemistry 2011